



Contents lists available at ScienceDirect

Earth and Planetary Science Letters

journal homepage: www.elsevier.com/locate/epsl

Expression of the Early Toarcian negative carbon-isotope excursion in separated carbonate microfractions (Jurassic, Paris Basin)

Michaël Hermoso^{a,*}, Laurence Le Callonnec^a, Fabrice Minoletti^a, Maurice Renard^a, Stephen P. Hesselbo^b

^a UPMC Univ Paris 06, JE 2477 Biominéralisations et Paléoenvironnements, Case Postale 116, 4 place Jussieu, 75252 Paris Cedex05, France

^b University of Oxford, Department of Earth Sciences, Parks Road, Oxford OX1 3PR, United Kingdom

ARTICLE INFO

Article history:

Received 22 March 2008

Received in revised form 6 October 2008

Accepted 18 October 2008

Available online 28 November 2008

Editor: M.L. Delaney

Keywords:

Early Toarcian

Oceanic Anoxic Event

carbon isotope

calcareous nannofossils

diagenesis

ABSTRACT

The causes of the pronounced negative excursion in carbon-isotope values that was recorded during the Early Toarcian Oceanic Anoxic Event (T-OAE) are still under debate, particularly with regard to the local versus global pattern of the excursion, and the extent to which recorded signals are under a diagenetic control. In this study we employ a novel microseparation technique in order to investigate the isotopic and mineralogical characteristics of different size fractions of the carbonate content from a Toarcian section recovered from the Sancerre–Couy borehole, southern Paris Basin. Beyond the recognition of a -6% $\delta^{13}\text{C}$ excursion in the bulk carbonate content, our data also demonstrate that biogenic particles (such as coccoliths) and inorganic grains precipitated as early diagenetic phases (including dolomite) both record the excursion with the same magnitude. Although several black shales occur through the Paris Basin Toarcian section, it is only that associated with the onset of the OAE that coincides with a large negative carbon-isotope excursion. Taken together these observations indicate that during this event, the entire water column was characterized by homogeneous carbon-isotope values; such a pattern is incompatible with the idea that the negative excursion was generated simply through the upwelling of bottom waters enriched in re-mineralized organic carbon (cf. “the Küspert model”), since this would have required a strong vertical gradient in the water column. Additionally, the Paris Basin data show that the decrease in carbonate $\delta^{13}\text{C}$ values during the OAE occurred in several discrete steps (each of some -2%), as has previously been found for organic carbon substrates in other European sections. The stepped nature of the isotopic profile, which is part of a stratigraphic signature previously ascribed to Milankovitch forcing, is compatible with regular pulsed input of light carbon into the whole atmosphere–ocean system from a climatically sensitive source such as gas hydrate, or from thermal methanogenesis of organic-rich sediments in the Karoo–Ferrar large igneous province. Contrasts in the amplitude of the negative carbon-isotope excursion on a regional scale remain an important unexplained aspect of the Toarcian record.

© 2008 Elsevier B.V. All rights reserved.

1. Introduction

Oceanic anoxic events (Schlanger and Jenkyns, 1976) correspond to periods of increased organic matter fossilization (i.e. huge ^{12}C trapping) during which the carbonate carbon isotopic ratio is relatively high (up to 2% as expressed in $\delta^{13}\text{C}$). However, some anoxic periods display very sharp negative shifts in the carbon isotope profiles (Scholle and Arthur, 1980; Renard, 1985; Weissert and Channell, 1989; Clarke and Jenkyns, 1999; Erba et al., 1999; Hesselbo et al., 2000; Jenkyns, 2003; Weissert and Erba, 2004; Renard et al., 2005) leading to primary $\delta^{13}\text{C}$ values less than -1% .

During the Early Toarcian OAE, $\delta^{13}\text{C}_{\text{carb}}$ increased: the values are around -1% to -2% at the base of the middle *tenuicostatum* Zone up to $+3$ or $+4\%$ in the *falciferum* Zone (Jenkyns, 1988; Jenkyns and Clayton, 1997; Jones and Jenkyns, 2001; Röhl et al., 2001; Jenkyns et al., 2002; Duarte et al., 2003; Kemp et al., 2005; Emmanuel et al., 2006; Hesselbo et al., 2007a; Woodfine et al., 2008; Sabatino et al., in press). Disrupting this positive trend, a pronounced negative isotopic shift has been described in marine carbonates, phytoplanktonic organic matter and organic biomarkers (Schouten et al., 2000; Van Breugel et al., 2006), and also in fossil wood which monitors the atmospheric C-isotope composition (Hesselbo et al., 2000, 2007a).

These isotopic decreases, occurring during relatively brief time (about 150 ky for the Early Toarcian, according to Suan et al., 2008a), are still difficult to explain. Recycling of remineralized carbon from deepest ^{12}C -rich water of an intermittently stratified seawater as originally proposed by the “Küspert model” (Küspert, 1982; Jenkyns, 1988; Sælen et al., 1996; Schouten et al., 2000) has been thought to be

* Corresponding author. Present address: University of Oxford, Department of Earth Sciences, Parks Road, Oxford OX1 3PR, United Kingdom. Tel.: +44 1865 272010.

E-mail address: Michael.Hermoso@earth.ox.ac.uk (M. Hermoso).

responsible for the record of such negative excursions in the sedimentary record, as such events occur in modern fjords (Van Breugel et al., 2005). Because a negative shift is recorded from limestones representing lithofacies in platform strata in westernmost Tethys, they also have been interpreted in terms of carbonate diagenesis (Jenkyns and Clayton, 1997). Rapid sea-level fluctuations in such shallow epicontinental environments have also been postulated to drive both $\delta^{13}\text{C}$ records in carbonate and phytoplanktonic organic matter (Röhl et al., 2001; Schmid-Röhl et al., 2002).

The observation of an apparently synchronous negative carbon isotope shift in Early Toarcian strata, and similarities to the well-documented Late Palaeocene event (Dickens et al., 1995), led Hesselbo et al. (2000) to consider methane hydrate dissociation as a plausible interpretation for the C-isotope negative excursion. One problem with this interpretation is the storage and causes of destabilization of methane hydrates within the European realm, because these compounds are only stable within a restricted range of temperatures and pressures that seem not compatible with warm climate of Early Jurassic times (Emmanuel et al., 2006; Beerling and Brentnall, 2007), although it is possible that methane hydrates were stored in higher latitudes.

A number of recent papers have questioned the global nature of the T-OAE and the $\delta^{13}\text{C}$ negative excursion (Van de Schootbrugge et al., 2005; Wignall et al., 2006; McArthur, 2007) based on belemnite carbon-isotope profiles, which do not clearly record the negative shift. Van de Schootbrugge et al. (2005) argue that a deep-water upwelling event is more appropriate to explain the C-isotope excursion, similarly to the Küspert model. Also on the basis of belemnite data, Jiménez et al. (1996), Rosales et al. (2001), and Bailey et al. (2003) have postulated that Toarcian bulk carbonates have not retained their pristine geochemical composition due to the burial diagenesis. Other authors have suggested that some profiles that do not show the negative carbon isotope excursion should be taken at face value and indicate that the negative excursion did not occur everywhere (e.g. McArthur, 2007). However, poor sample resolution, incomplete sedimentary record and uncertainty about the nature of carbonates in these sections may equally well explain such observations (e.g. Hesselbo et al., 2007b).

The aim of this work is to investigate the individual C-isotope characteristics of different carbonate components in a key Toarcian succession using an innovative micro-separation protocol. We have chosen to study the sedimentary and geochemical evolution of the Paris Basin because no high-resolution study has yet been published for this location in spite of an abundant literature on organic geochemistry. In the southernmost part of this basin, the Sancerre–Couy drill core (Cher, France) provides a high sedimentation rate reference section for the Toarcian strata of the Paris Basin, and allows a detailed analysis of the negative $\delta^{13}\text{C}$ excursion.

2. Geological settings of the Early Jurassic Paris Basin

During the Early Jurassic, extensional tectonics of the European realm created a seafloor morphology characterized by shoals delimiting subsiding shallow basins. The Paris Basin is one such basin in a restricted epicontinental sea (Fig. 1), and corresponds to a Boreal faunal realm where organic matter was better preserved than in more oxygenated Tethyan deposits (Bassoulet and Baudin, 1994). Palaeoclimatic reconstructions (Baudin et al., 1990; Chandler et al., 1992; Bailey et al., 2003) indicate a warm and wet climate in NW-European basins, in agreement with their subtropical 30°N palaeolatitude (Bassoulet et al., 1993).

At this time, the Toarcian biosphere underwent important changes, with extinctions affecting marine and continental life (Hallam, 1983, 1996; Bassoulet and Baudin, 1994; Harries and Little, 1999; Macchioni and Cecca, 2002), including significant overturns in the calcareous nanoflora (Mattioli et al., 2008). The causes of these crises were likely

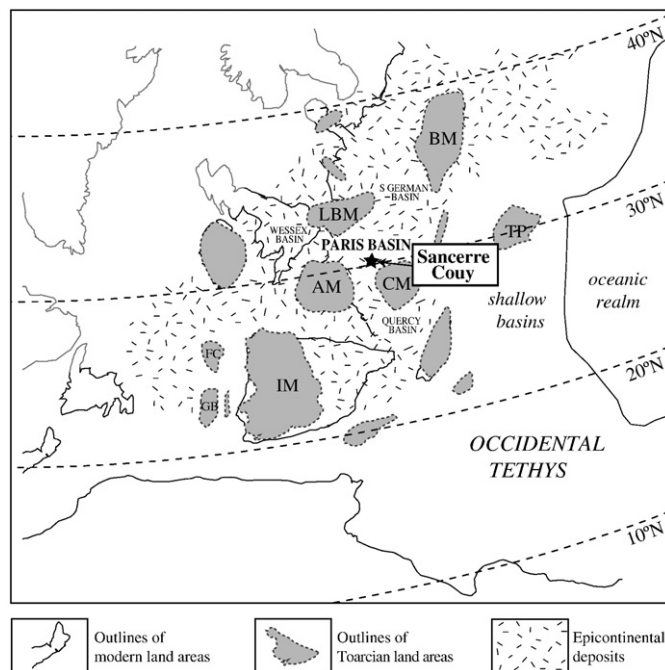


Fig. 1. Palaeogeographic map for the Toarcian in NW Europe showing the Sancerre–Couy borehole location (modified after Bassoulet et al., 1993). Emerged lands are in grey tint (BM: Bohemian Massif, LBM: London-Brabant Massif, AM: Armorican Massif, CM: Central Massif, FC: Flemish Cap, GB: Galicia Bank, IM: Iberian Massif, TP: Tisza Plate).

due to the conjunction of palaeoceanographic factors such as sea level rise and/or poorly oxygenated seawater (Jenkyns, 1988) and/or intense volcanic activity related to the Karoo–Ferrar large igneous province emplacement (Pálfi and Smith, 2000; Wignall, 2001; cf. Gröcke et al., accepted for publication). This peculiar framework also explains the onset of a Oceanic Anoxic Event, so-called ‘Posidonienschiefer Event’ (Jenkyns, 1988; Jenkyns et al., 2002), which has been linked with high volcanic emissions, enhanced continental leaching (Cohen et al., 2004), and a second-order maximum transgression corresponding to the maximum flooding onto the NW European epicontinental surface (Hallam, 2001).

The Sancerre–Couy borehole is located in central France (Fig. 1), near Bourges city. It was drilled in 1986–1987 for studying the magnetic anomaly of the Paris Basin (program GPF ‘Géologie Profonde de la France’, Lorenz, 1987). The borehole has provided continuous recovery from Carboniferous up to the Middle Jurassic strata. The Toarcian sediments occur between 355.50 and 198.30 m depth and were fully recovered (albeit with localized drilling disturbances). The studied interval (Late Pliensbachian *spinatum* Zone to Early Toarcian *falciferum* Zone) is 20 m thick.

The biostratigraphic framework (Fig. 2) is described by Gély et al. (1996). The Pliensbachian–Toarcian boundary is placed at 355.50 m with confidence. However, the transition between *tenuicostatum* and *falciferum* Zones is imprecisely defined due to a scarcity of index fossils. Nevertheless, the biostratigraphic boundary is approximately placed at 344.50 m. The sediments are mainly composed of detrital minerals (illite, chlorite and quartz) mixed with various calcareous particles. Black shales occur between 348 and 307 m at this location (Lorenz et al., 1991). In the studied section, three distinct black shale intervals are observed, they are disrupted by bioturbated marls with low organic content (Fig. 2).

3. Material and methods

As the bulk carbonate content is the mixture of various calcareous particles (coccoliths, calcareous dinoflagellates, inorganic

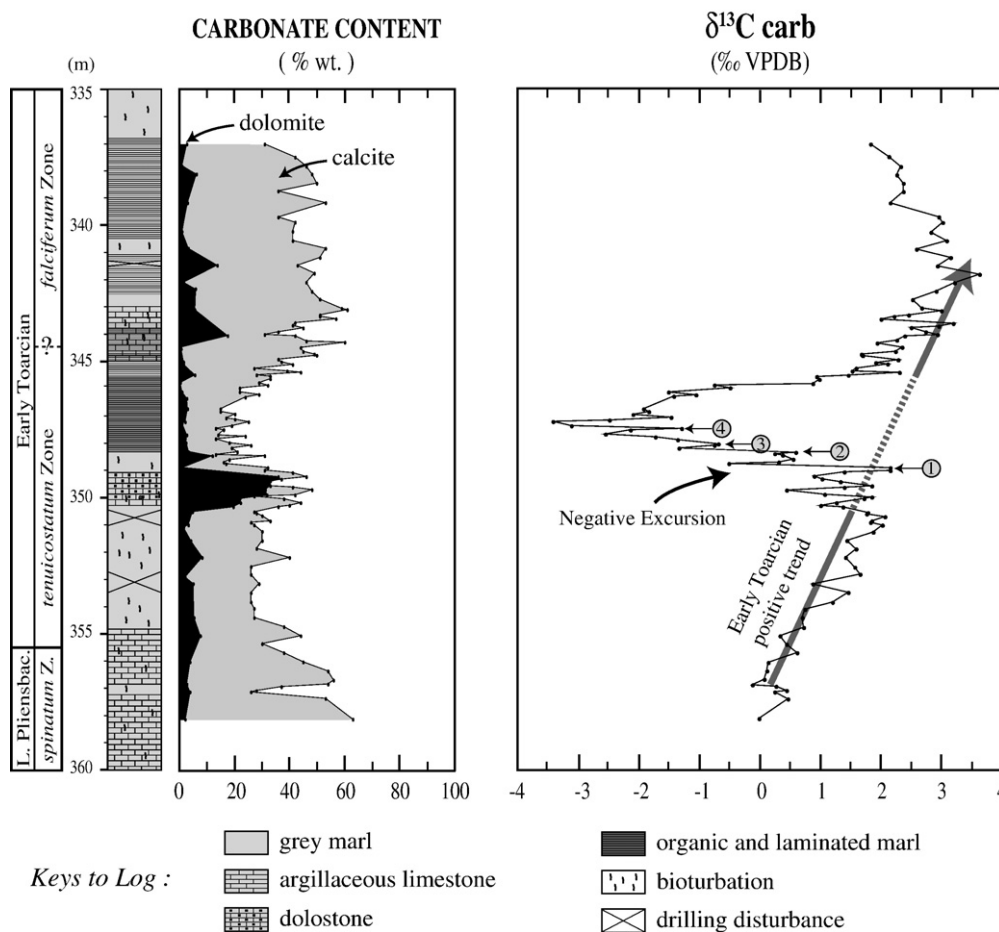


Fig. 2. Mineralogical (total carbonate content and relative proportions of calcite and dolomite) and stable C-isotope ratios of bulk carbonate through the studied interval. The biostratigraphic framework is from Gély et al. (1996). Encircled numbers correspond to the four steps described in text. BS1, BS2 and BS3 show the three black shale intervals disrupted by bioturbated sediments observed in this section.

precipitations, etc.) that have distinct origins, it is of primary importance to access their specific geochemical signature. For that, we have first identified each particle type (coccoliths, calcispheres, nannoliths, rhombs, anhedral monocrystals) and then isolated them according with their sizes and physical resistances. The aim was to i) estimate the primary validity of isotopic measurements performed on bulk carbonate and ii) reconstruct specific geochemical curves (i.e. coccolith signal) and to compare them to the bulk carbonate evolution.

3.1. Granulometric separation of sedimentary particles

The separation of sedimentary particles was carried out by applying a size-grading separation protocol (Minoletti et al., 2001, in press). This technique enables isolation of micrometric fractions differing in size and physical strength. About 10 g of sediments were first gently crumbled and put into a surface active solution (Benzalkonium Chloride solution) to eliminate rock aggregates, enable the dispersion of clay minerals, and ease the subsequent filtering steps. Then, a preliminary separation step was performed with a 20 μm sieve to retain resistant aggregates and microfossil fragments. The corresponding filtrate consists of a suspension containing all the <20 μm separated particles of the bulk sample.

3.1.1. Concentration of nannofossils from bulk sediments

A semi-quantitative evaluation of size ranges and total abundance of calcareous particles smaller than 20 μm was performed

in order to select the appropriate following filtration steps. This enables recovery of fractions that contain only one dominant component (>80%) from polygenetic assemblages (bulk sample). The fine fractions (<12 μm) were separated using polycarbonate membrane filters.

Samples were selected according to the geochemical signatures of bulk carbonate and the composition of calcareous assemblages. They were separated with similar steps of filtration: 20 μm , 10 μm , 8 μm , 5 μm , 2 μm . Each filtration step was accompanied by smear-slide observation in order to check the granulometric homogeneity of the fractions. After separation, they were dried, weighed and analyzed. Nannofossil-rich fractions were obtained in the size range of these particles, mainly between 2 and 8 μm .

3.1.2. Purification of monocrystalline fractions using strong ultrasonic treatment

Fifteen samples were purified into calcareous monocrystalline particles (dolomitic rhombs and calcitic macrocrystals). These fractions were obtained using the resistance of monocrystalline structures to strong ultrasonic treatment, while polycrystalline ones (such as biogenic particles) are fragmented. This treatment was done using a very powerful ultrasonic bath operating over several hours.

After this particle disassembly step, all samples were recovered through a 5 μm membrane. Since nannofossils are sensitive to cavitation induced by the ultrasonic supply, they are broken up into <5 μm particles. Retentates were optically checked for their homogeneity.

3.2. Characterization of the separated calcareous assemblages

In order to properly compare carbonate assemblages, smear-slides were made from homogenized suspension containing 60 mg of sample in 60 mL neutralized water. Counts were performed using a high-resolution cross-polarized Zeiss optical microscope (magnification 1500). Some selected samples were investigated with a scanning electron microscope (SEM) coupled with a micro-probe device in order to: i) characterize precisely the sedimentary components, ii) confirm the mineralogy of calcareous particles deduced from optical observations and perform spot chemical measurements on these particles, and iii) observe potential dissolution and recrystallization features of these calcareous particles. The composition of calcareous assemblages of the separated fractions was evaluated using optical and electronic observations and X-ray semi-quantification. This enables quantification of the respective proportions of dolomite and calcite, and assessment of the composition of calcitic fraction (coccoliths, *Schizosphaerella*, monocrystals) in terms of dominant particles.

The mineral phases of the sediment were identified by X-ray diffraction using a Bruker D-501 X-ray diffractometer (CuK α , Ni filtered radiation) coupled with an automated DACO-MP system. Scans were performed from 3° to 75° at a scanning speed of 0.05° 2 θ /s, with counting steps of 1 s. Semi-quantitative measurements of carbonate mineral abundances (calcite versus dolomite) were realized on non-oriented powdered samples. Intensity of the main peaks (104) of calcareous phases was corrected according to its respective 'I/corr' factor' as given by the International Centre for Diffraction Data (ICDD) in the Powder Diffraction File (PDF) database. Corrections applied were 2.00 for the calcite diffracting between 3.035 and 3.025 Å, and 2.35 for the dolomite at about 2.91 Å.

3.3. Carbon-isotope analyses of calcareous phases

Through this Late Pliensbachian–Early Toarcian interval, bulk samples (120) and granulometric fractions (20) were analyzed for their C and O stable isotope ratios ($\delta^{13}\text{C}$ and $\delta^{18}\text{O}$) using a SIRA 9 mass spectrometer. The extraction of the CO₂ was realized from ~10 mg powdered sample by reaction with purified orthophosphoric acid at 50 °C for 15 min. The purification of CO₂ was performed using cryoscopic traps (liquid nitrogen followed by carbonic ice). The results are expressed in ‰, relative to the VPDB international standard. The precision of the measurements is $\pm 0.05\%$ PDB for the carbon isotope ratio. The oxygen-isotope dataset is given as supplementary material in the online version.

4. Results

4.1. Lithofacies and composition of the sediments

The Late Pliensbachian deposits (360 to 355.50 m) consist of grey, bioturbated argillaceous limestone (Fig. 2). The carbonate content is about 50 to 60% and displays a steady decrease (down to 30% at 354.50 m). Detrital minerals are represented by clays (illite and chlorite) and quartz. The pyrite phase mainly consists of disseminated framboids.

The lower part of the Toarcian strata (355 to 350.50 m) is composed by bioturbated marls with moderate carbonate contents (25–30%). This monotonous marly succession is succeeded by a calcitic dolostone between 350.35 and 349.22 m. The carbonate content is up to 60% and comprises ferroan dolomite (40%) in large dolomitic rhombs (Figs. 3, 4A) and calcite (20%). In this level, pyrite is also expressed in its octahedral habit with large crystals up to 20 μm . Above 349 m, the carbonate content thus shows a significant decrease (down to 20%), and the carbonate phase is mainly composed by calcite (70% wt.).

A 2-m thick, dark, and laminated interval is observed between 348.32 and 345.50 m comprising alternations of dark (organic matter, pyrite) and pale (quartz, calcite) laminae which are characteristic of the Schistes carton Formation as described by Röhl et al. (2001), and Bour et al. (2007) for the easternmost Paris Basin. The carbonate content is low (15–20%) but shows a progressive increase from 347 m upwards. This interval contains large amount of phytoplanktonic organic matter reaching about 10% (e.g. at 346.90 m: TOC=10.4% and hydrogen index=649) associated with large amounts of framboidal pyrite (~4%).

At 345 m, these laminated deposits terminate and the strata return to grey bioturbated marls. Relatively high carbonate content is observed at about 343 m (55%). This upper part of the studied section (343–347 m) is marked by higher amounts of dolomite (20% of the whole carbonate), and other laminated black shales (Fig. 2) are again associated with higher pyrite content (2–3%). But in respect with the first anoxic interval (BS1, Fig. 2), it is not accompanied by a carbonate content decrease.

4.2. Evolution of the calcareous particle assemblages and preservation

4.2.1. Overview of calcareous particles

Throughout the studied interval, the main dominant carbonate components are calcareous nannofossils and, to a lesser extent, carbonate monocrystals (dolomitic rhombohedra and anhedral calcitic particles). A few microfossils (foraminifera and ostracods) and

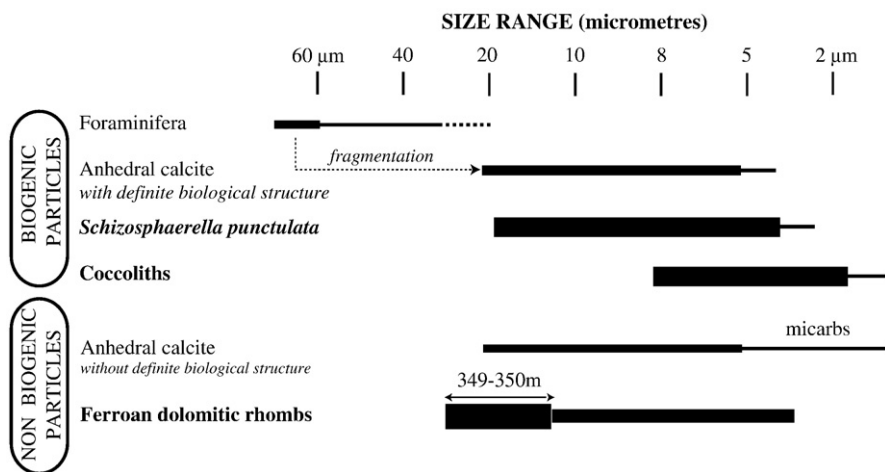


Fig. 3. Typology and size range of calcareous particles observed through the studied interval. Thick line indicates that these particles are dominant. Thin line corresponds to accessory amounts. Dotted line used when only debris are observed.

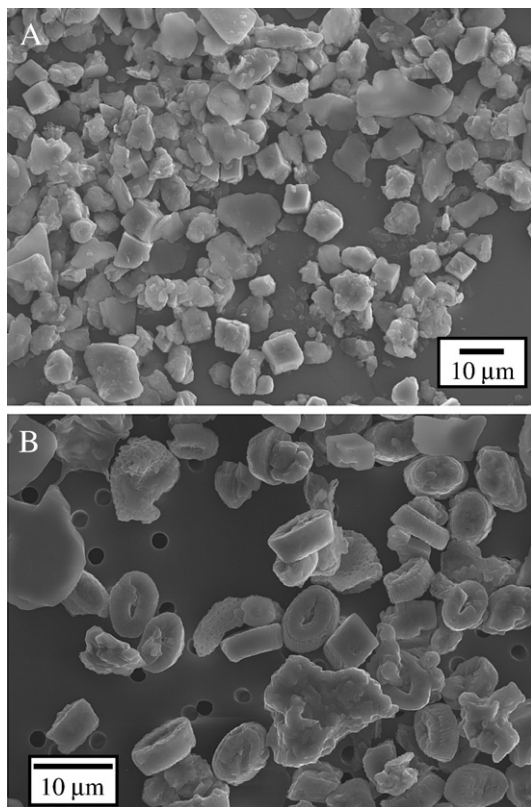


Fig. 4. SEM micrographs of granulometric fractions. A: Dolomitic rhombs-rich assemblage (349.22 m–8 to 12 μm). B: Example of a coccolith-rich assemblage in which *Crepidolithus crassus* is obviously the main taxa here (339.10 m–fraction 5 to 8 μm). Scale bars are 10 μm .

echinoderm spines are found in bioturbated levels but their contribution to the bulk carbonate can be disregarded (<1 wt. %). Moreover, they are totally absent in the organic-rich interval. The size spectra and abundance in bulk carbonate of each calcareous component are given in Fig. 3.

The calcareous nannoflora is mainly represented by two coccolith taxa, *Crepidolithus* (Fig. 4B) and *Lotharingius* genera, and two nannoliths, *Schizosphaerella punctulata*, assigned to calcareous dinoflagellates by Kålin and Bernoulli (1984), and the *Incertae sedis* *Orthogonoides hamiltoniae* of uncertain biological affinity. The ecological preferences of Early Jurassic calcareous nannofossils are unclear but in comparison to modern coccoliths and calcareous dinoflagellates, are interpreted to thrive within photic zone waters.

Two different types of carbonate monocrystals are found in the studied interval: euhedral rhombs and anhedral crystals (Fig. 3). In addition to their distinct morphologies, they can be distinguished by their birefringence colours under cross-polarized light (iridescent and light brown respectively). The SEM spot analyses confirm that these two monocrystal types correspond to distinct mineralogies and chemical compositions as well: anhedral crystals are calcitic with low Mg substitution whereas rhombs are Fe-rich dolomite isotypes (from ferroan dolomite toward ankerite).

4.2.2. Evolution of calcareous assemblages

Beneath the dolomitic interval (350.35 m), relatively small coccoliths such as *Biscutum* and *Schizosphaerella* calcispheres are the main calcareous contributors to the bulk carbonate. Other calcareous components are dolomite rhombs (Fig. 4A) and some calcitic monocrystals. In this interval, the abundance of Mg- and Fe-rich rhombs progressively increases from less than 5% up to 20%.

In the dolomitic interval (350.35 to 349.22 m), Mg- and Fe-rich rhombs becomes the principal calcareous components of the samples.

The relative abundances of calcareous nannofossil taxa does not significantly change, but their total abundances are relatively lower due to the dominance of ferroan dolomite crystals.

In the low-carbonate interval (348.50 to 346.00 m), the carbonate is again dominated by calcareous nannofossils. The nannolith *Orthogonoides hamiltoniae* becomes more abundant, which contrasts with its very low abundance in the rest of the studied interval. Foraminifera are totally lacking and the proportion of dolomite is notably low (<10% weight in the bulk carbonate).

In the upper part of the section, the carbonate content increases along with the abundance of thick coccoliths such as the *Crepidolithus* murolith that dominates the calcareous assemblage (Fig. 4B) according to previous observations in the western Tethys (Mattioli et al., 2008). At the same time, the dolomitic content decreases upwards but is highly variable (between 45% at 344.07 m and 37% at 341.46 m).

4.2.3. Calcareous nannofossil preservation

The studies of Goy (1979) and Bour et al. (2007) have highlighted a good preservation of calcareous nannofossils in Early Toarcian black shales of the Paris Basin. In Sancerre, the same preservation pattern is observed throughout the studied interval. Pristine biological structures of calcareous nannofossils (coccoliths and dinoflagellate calcispheres) are always clearly evident despite slight etching of shields and central areas (Fig. 5). In the organic-rich horizons (348.32 to 345.50 m; 347.50 to 341 m; 340.5 to 339 m; resp. BS1, BS2 & BS3 in Fig. 2), enhanced dissolution features are observed on coccoliths, but the preservation remains rather good. Nonetheless, a 10 cm-thick interval (347.40–347.30 m) in which the carbonate content is very low (~15%), with maximal total organic carbon contents (about 10% TOC) displays poorer preservation.

Even if calcite dissolution intensity is variable, SEM imaging carried out throughout the whole interval points out the absence of overgrowth on calcareous nannofossils, even in the organic-rich and dolomite-rich intervals (Figs. 4A, 5). Noël and Busson (1991) have demonstrated the high susceptibility to recrystallization of *S. punctulata* because of the hollow microstructure of their tests. In Sancerre, this taxon never displays any secondary calcite infilling in the shell porosity (Fig. 5). Primary test microstructure is always evident.

4.3. Isotopic results

4.3.1. Bulk carbonate C-isotope evolution

The Sancerre–Couy sediments record a significant positive trend of the $\delta^{13}\text{C}$ during the Early Toarcian from 0.5 to 3.5‰, corresponding to a 3‰ increase in magnitude (Fig. 2). During the *tenuicostatum* Zone, this trend is sharply disrupted by a pronounced negative excursion (–6‰ in magnitude). After that, the $\delta^{13}\text{C}$ returns to its long-term positive trend.

In detail, from the bottom of the studied interval up to 350.50 m, a gradual increase from 0‰ to 2‰ is observed in the bulk carbonate $\delta^{13}\text{C}$ evolution. The dolomite-rich level records isotopic values slightly lower (1.5‰ in average, minimum value: 0.43‰ at 349.70 m) than those observed in the underlying marls, whereas the calcareous assemblage is significantly different. The negative excursion of the carbon-isotope is recorded from the top of the dolomite-rich limestone bed (349 m). This negative shift occurs in four steps, each of which records a –2‰ decrease in magnitude (348.90, 348.32, 347.99, 347.35 m, Fig. 2), separated by short increases in $\delta^{13}\text{C}$ values (0.5 to 1‰). After the most negative isotopic value (347.20 m, $\delta^{13}\text{C}$ = –3.43‰), the positive trend of the $\delta^{13}\text{C}$ is resumed over a short stratigraphic interval. Similar values to those observed underneath the dolomitic level (~2‰) are observed at about 345 m. The $\delta^{13}\text{C}$ evolution goes then back progressively to the positive trend observed for the lower part of the Early Toarcian age deposits. The maximum value at 341.77 m (3.6‰) is followed by a progressive decrease (2‰ in

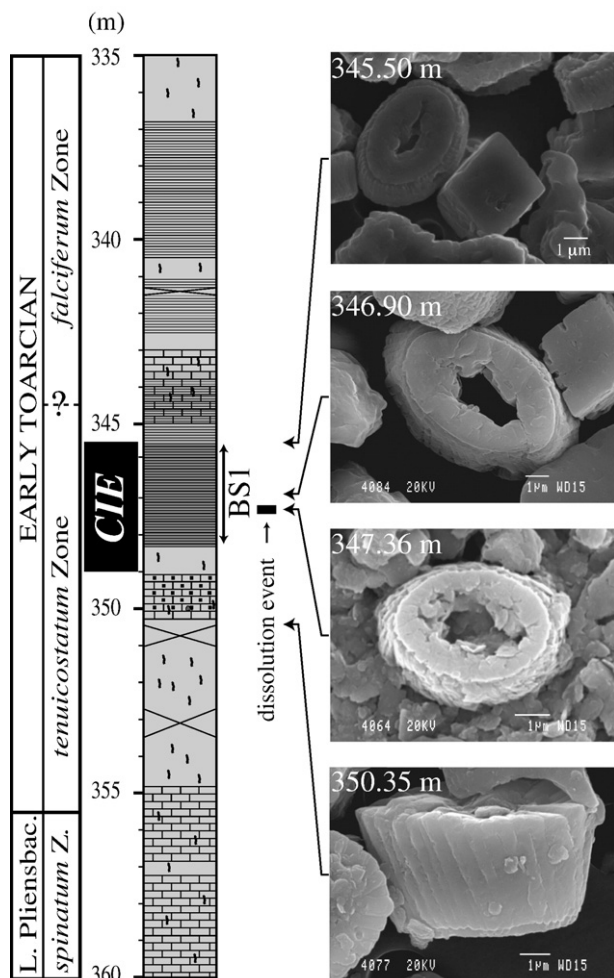


Fig. 5. Representative SEM micrographs of coccoliths across the first black shale level (BS1; 348.32 up to 345.50 m). Note the relatively poor preservation at 347.36 m corresponding to the dissolution event (sensu Mattioli et al., 2004), recorded in Sancerre between 347.40 and 347.30 m. Other levels display better preservation. Throughout the whole interval, recrystallization features are absent from all coccoliths investigated by SEM imaging. Note also the offset between the inception of C-isotope negative excursion (CIE; black box) and the first anoxic stage (BS1).

magnitude) in the upper part of the *tenuicostatum* Zone and in the *falciferum* Zone.

4.3.2. Biogenic particle geochemistry

The finest calcareous fraction of the sediment ($<8 \mu\text{m}$) is composed of a mixture of nannofossils and monocrystals with a low contribution of 'micarbs' ($<5 \mu\text{m}$ calcareous particles, see definition and discussion in Minoletti et al. (2008)). The $<2 \mu\text{m}$ fraction compositions are hard to assess due to very low carbonate contents ($<10\%$) and the difficulty in identifying small particles in the smear-slides in clay-rich material. Biogenic particles are usually concentrated into the 2 to 5 μm fraction (small coccoliths such as *Biscutum* or *Lotharingius*), and the 5 to 8 μm fraction with bigger coccoliths such as *Crepidolithus* and *S. punctulata* calcispheres (Fig. 4B). The composition of each fraction in terms of calcareous assemblage is reported in Fig. 6 (dolomite versus calcite of the whole calcareous fraction, and the main contributor to the calcitic part).

The Early Toarcian positive trend of the carbon-isotope ratio is recorded in all these fractions whatever their calcareous particle contents. Both granulometric fractions (2–5 and 5–8 μm) of each level treated have near similar $\delta^{13}\text{C}$ signatures, except for the 354.17 m level ($\Delta\delta \sim -1\%$) which shows a lighter C-isotope signature for the 5–8 μm fraction. For the low $\delta^{13}\text{C}$ bulk signatures (347.40 and 346.90 m samples), in spite of the low carbonate contents, calcareous particles of the 2–5

and 5–8 μm fraction are biogenic-dominated and record the bulk negative shift of the $\delta^{13}\text{C}$. Geochemical analyses indicate that these fractions are close to their respective bulk carbonate signatures. These differences are less than 0.5‰ in magnitude. For the 347.40 m level, even if the composition of the 2 to 5 μm fraction is dominated by monocrystals, its $\delta^{13}\text{C}$ signature is yet close to the bulk signature (Fig. 6).

4.3.3. Non-biogenic carbonates

Monocrystal-rich fractions enable measurement of the specific geochemical signatures of the $>5 \mu\text{m}$ calcareous monocrystalline particles (anhedral calcite and dolomite rhombs, Fig. 4A) reflecting the chemistry of their growth environments. The $\delta^{13}\text{C}$ signatures of these fractions follow the bulk record evolution, especially during the negative excursion with the same magnitude of -6% (Fig. 6). In detail, these particles record lighter C-isotope ratios in $\delta^{13}\text{C}$ carbonate than the bulk (average range of 0.5‰), except during the isotopic event. These monocrystalline calcareous particles thus record the $\delta^{13}\text{C}$ negative excursion with the same magnitude as the bulk carbonate, in spite of their low abundance in the whole calcareous assemblage and their different nature.

5. Discussion

5.1. Preservation of pristine geochemical signals in biogenic calcite

Dissolution is not likely to modify the isotopic and elementary composition of coccolith plates because their near-instantaneous bioprecipitation in the coccolithosome (Paasche, 2002) ensures a chemical homogeneity. In the context of black shale deposition, organic matter decay occurring during early burial is responsible for carbonate dissolution due to the release of acidic products in the interstitial environment (Suess, 1970; Müller and Suess, 1979). Dissolution process can explain the relatively poor preservation state of biogenic calcite in organic-rich intervals, particularly when organic content is very high like in the most dissolved coccolith assemblage (347.40–347.30 m). In Sancerre, a further convincing argument indicating that C-isotope negative values are not linked with the dissolution process, relies on the fact that the onset of the negative excursion (i.e. between the first and second steps) is recorded in well preserved coccolith assemblages in bioturbated facies. Aside from this diagenetic process, seawater acidification during the C-isotope negative excursion has also been postulated to explain differential preservation indexes (Mattioli et al., 2004; Erba, 2004). For these authors, this 'alkalinity alteration' of seawater is the consequence of dramatic increase in CO_2 concentration in the ocean. Nevertheless, the respective contributions of these two distinct processes are difficult to assess.

A more striking parameter for understanding the geochemistry of coccolith-bearing successions is the recrystallization developed on calcareous nannofossils. Secondary carbonate grown on calcareous nannofossils, if present in sufficient quantity, is likely to distort their primary geochemical signal. In Sancerre, such carbonate precipitation is not apparent through either optical or SEM observations (Figs. 4, 5). When the sediment accumulation rate is low, microbial-derived carbonate can precipitate in the sulphato-reduction zone (Bréhéret et al., 2004), but this feature is restricted to nodules that are not observed in Sancerre. Thus the good preservation of geochemical signatures of biogenic particles can be inferred with confidence and nannofossil-rich fractions can be considered as reliable monitors of the chemical evolution of the photic zone. Even if dissolution seems to be enhanced throughout the C-isotope negative excursion, and at a larger scale in the three organic-rich intervals, calcite or dolomite recrystallization did not significantly occur. Furthermore, the high organic content in this interval probably hampers subsequent carbonate recrystallization.

As a consequence, since calcareous nannofossil fractions record the C-isotope negative excursion, this strongly supports the notion

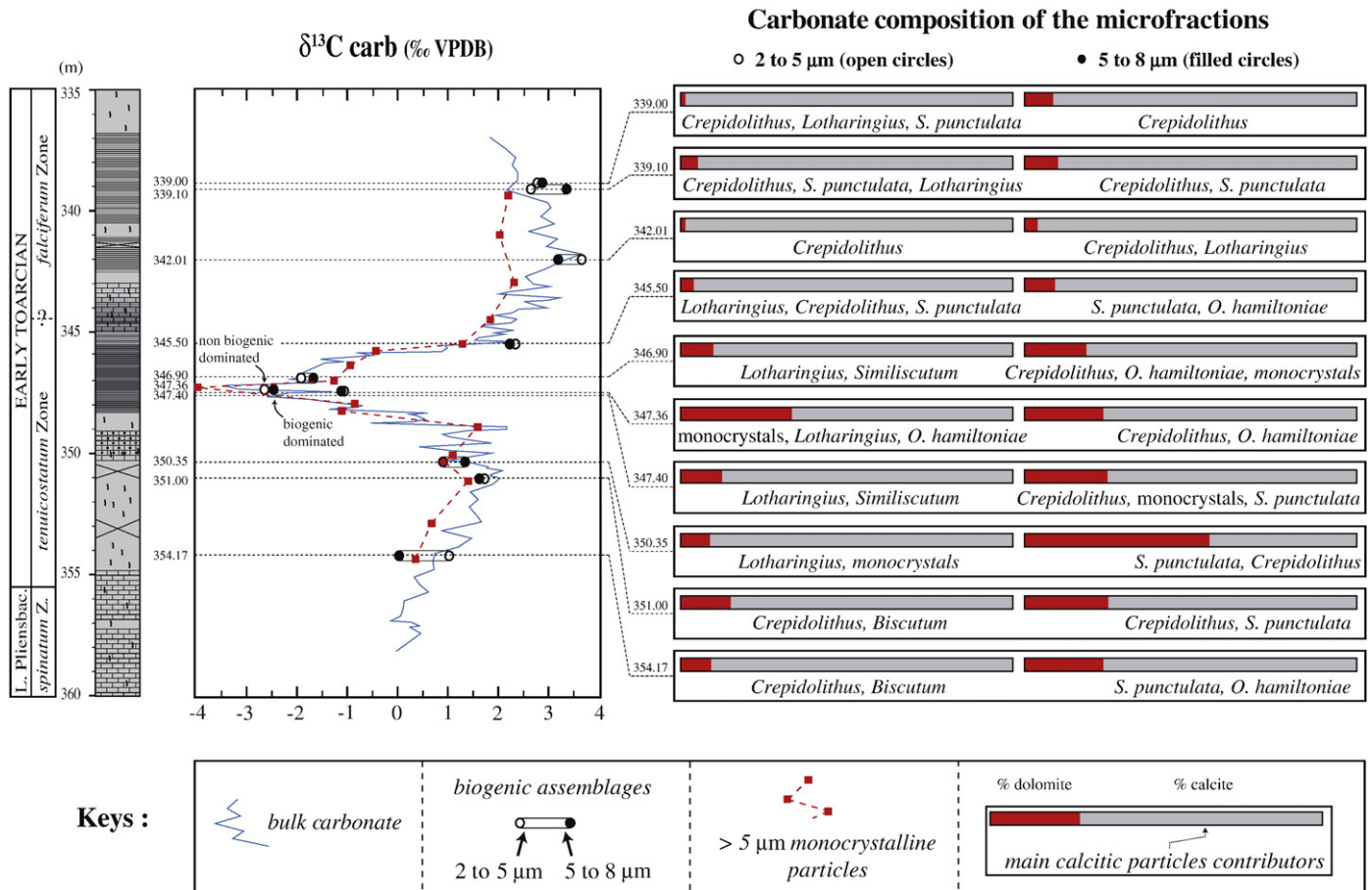


Fig. 6. Comparison between isotopic evolution of bulk carbonate (thin line) and separated carbonate fractions (filled circles: 2–5 μm fractions, open circles: 5–8 μm fractions and filled squares: > 5 μm calcareous monocrystalline assemblages). On the right: Calcareous composition of each 2–5 μm and 5–8 μm fractions. Sizes of filled boxes (dolomite) and grey boxes (calcite) indicate the relative abundance of these two carbonate phases (semi-quantification from XRD measurements). Underneath the boxes are the optical semi-quantitative evaluations of calcitic particle assemblages.

of a primary isotopic perturbation in the seawater with a $\delta^{13}\text{C}$ magnitude of $\sim -6\%$, at least in the photic zone where the nannoplankton thrive.

5.2. Calcareous nannofossil assemblages and biogeochemical insights

Isotopic offsets between biogenic fractions at a given stratigraphic level could be explained by distinct species-specific isotopic compositions. In the present dataset these differences are limited, generally lower than 0.7‰. The negative carbon-isotope excursion cannot be ascribed to the change in calcareous nannofossil assemblage, pointed out recently by Mattioli et al. (2008) in the western Tethys, because our data from separated fractions indicate closely similar isotope values whatever the assemblage composition. For the comparable PETM event, Stoll (2005) has demonstrated that changes in nannofossil assemblages could not have made a significant contribution to the negative carbon-isotope excursion in bulk carbonate due to known restricted differential vital effect in Palaeogene species.

5.3. Dolomite analyses for tracking bottom water chemical changes

Two main factors inhibit the precipitation of dolomite from seawater: i) the presence of sulphate ions, and ii) the hydration of the magnesium ions (Tucker and Wright, 1990). The formation of dolomite then involves diagenetic chemical processes. Two hypothetical origins are possible for the dolomite mineralization described in the present study. Firstly, an early diagenetic origin is possible, related

to reducing conditions in the sediment. Here, the precipitation of Mg- and Fe-rich carbonate occurs underneath the sulphate-reduction/methanogenesis interface. At this level the sulphate ions have been reduced during pyrite formation. Secondly, during later diagenetic sediment compaction, Mg- and Fe-rich fluids may be expelled from clay-rich sediments. Mg- and Fe-rich carbonates could then have precipitated from these fluids, which are not in equilibrium with seawater. The morphology of such monocrystals should correspond to cast fillings (Mélières, 1991). In the Sancerre–Couy core, an early diagenetic origin is most realistic: the relatively high amount of framboidal pyrite attests to an early reducing diagenetic environment in the sulphate reduction environment. Similar early diagenetic phase (dolomite rhombs) has been found in ODP Leg 172 sites in the North Atlantic by Çagatay et al. (2001) or on the Peru margin, sampled during ODP Leg 201 expedition (Meister et al., 2006).

Except in the dolostone interval between 350 and 349 m, calcitic anhydrous monocrystals and dolomite rhombs are never the main component of the calcareous assemblage, and through the interval of the negative excursion the amount of the early diagenetic carbonate is lower than in the underlying and overlying marls. The evolution of carbon-isotope signatures in the monocrystal carbonates is closely linked to that of the bulk carbonate in spite of their low mass contribution to the whole bulk signal. An explanation of the carbon-isotope excursion in bulk carbonate in terms of diagenesis is thus untenable. Further evidences that bottom waters had very similar carbon-isotope values as surface waters, has been provided recently by Suan et al. (2008b) who show that brachiopod carbon-isotope

values track bulk carbonate carbon-isotope values in the section at Peniche, Portugal.

5.4. Implications for understanding the Toarcian C-isotope negative excursion

Reutilization of carbon of organic origin via upwelling deep water has previously been suggested to explain the negative excursion commonly observed in marine organic matter in European sections as explained by the Küspert model (Küspert, 1982) and quoted more recently by Van de Schootbrugge et al. (2005), Wignall et al. (2006) and McArthur (2007). However the data presented here strongly suggest a carbon-isotope homogeneity through the water column that is incompatible with the idea of upwelling of deep waters with a distinctly different isotopic composition from those at the surface. Furthermore, otherwise similar black shale facies in the overlying parts of the *falciferum* zone do not show the negative carbon-isotope excursion (Fig. 2). The excursion is peculiar to the age of the sediment, not its depositional setting. An organic geochemical study of Toarcian core material from the eastern Paris Basin by Van Breugel et al. (2006) has also cast doubt on the effectiveness of upwelling as a potential cause of the Early Toarcian negative carbon isotope excursion. These authors used the abundance of isorenieratane (produced by green sulfur bacteria and indicating photic zone anoxia) through the C-isotope negative excursion, together with the carbon-isotope values of this biomarker, to calculate the proportion of dissolved inorganic carbon remineralized during the negative shift in $\delta^{13}\text{C}$. They concluded that this source was insufficient to be responsible for the greater part of the C-isotope negative excursion as suggested by the Küspert model.

There has been considerable recent debate about the true magnitude of the carbon-isotope excursion at the PETM and thus the implication for the amount of isotopically light carbon that must have been introduced into the ocean and atmosphere compatible with inferred temperature change. In particular, data from Arctic drilling led Pagani et al. (2006) to suggest that the organic matter record more closely approximates the size of the carbon-isotope excursion in the total exchangeable carbon reservoir than does the size of the excursion in carbonates. Very similar considerations apply for the Toarcian (Cohen et al. 2007). In this case, it has been shown for several European sections that the size of the carbon-isotope excursion is consistent for marine and terrestrially derived carbon ($\delta^{13}\text{C}$ of about -6 to -7%), and that the excursion is about twice the size recorded from the best available carbonate record (Hesselbo et al. 2007a). Furthermore, we recognize for the first time the stepwise character of the C-isotope negative shift in phytoplanktonic carbonate record, as it has been previously highlighted in organic matter substrate (Jenkyns et al., 2001; Kemp et al., 2005). The consistency of values in organic material derived from different carbon-reservoirs is puzzling: if the excursion magnitudes have been inflated by processes such as soil moisture changes (cf. Bowen et al. 2004), then amplitudes in marine and terrestrial materials should be rather different from each other. The data from the present study show a primary excursion in carbonate of an equivalent magnitude to organic matter records; this fact, taken together with the demonstrated lack of diagenetic component or vital effect, strongly suggest a larger exchangeable reservoir excursion than has hitherto been appreciated, as for example by Beerling and Brentnall (2007) who used a magnitude of -5% for the carbon-isotope negative excursion in order to simulate the carbon budget required for this isotopic shift. It is then likely that they have underestimated the amount of carbon released into the atmosphere and the ocean. Some sections, as Peniche in Portugal (Hesselbo et al., 2007a), display a lower amplitude negative excursion in the bulk carbonate record, but the primary record (i.e. phytoplankton) seems not to be strictly maintained in this section (Mailliot et al., 2006). This should imply that the diagenesis is likely to lower primary isotopic shifts in some carbonate successions.

6. Conclusions

The carbonate record of the Toarcian OAE sampled from the southern Paris Basin is shown to comprise a mixture of biogenic and early diagenetic carbonate. Separated size fractions of the carbonate components all record the Early Toarcian negative carbon-isotope excursion with values closely similar to those obtained from bulk carbonate (-6%). The results indicate that the water column of the Paris Basin at this location was not characterized by a pronounced $\delta^{13}\text{C}$ vertical gradient with ^{12}C -rich bottom waters as necessitated by the Küspert model. Variety in the records of the Toarcian OAE across the European area was likely affected by regional parameters such as water column palaeodepth, redox state, and basinal restriction that pre-existed before this major palaeogeographic event. These factors can explain a relative diachronism of black shale deposition. Nonetheless, the subsequent anoxic pulses in this environment that lead to the deposition of several black shale levels in a longer-term time frame are not associated with other CIEs. This may exclude a local and environmental control of this isotopic event as supported by the “upwelling school”.

The good preservation of calcareous nannofossils in the southern Paris Basin enables the recognition of the stepped nature of this C-isotopic perturbation in diagenetic-screened carbonate material as previously demonstrated for the negative CIE of the PETM event.

As the size of the negative carbon-isotope excursion measured for this study in the southern Paris Basin is indistinguishable from that obtained from marine and terrestrial organic matter in other European sections, it has to be concluded that this largest carbon-isotopic excursion of Mesozoic times is the consequence of massive influx of isotopically-depleted carbon into the whole atmosphere–ocean.

Acknowledgements

The authors acknowledge the assistance of Nathalie Labourdette and Jean-Marc Hénot, (Université Pierre et Marie Curie, Paris), Abderhaman Toudert (Undergraduate research assistant) in the laboratory, and Omar Boudouma (Université Pierre et Marie Curie, Paris) and Norman Charnley (Oxford University) for SEM imaging. Marie-Madeleine Blanc-Valleron (MNHN, Paris) is warmly thanked for her assistance for quantifying carbonate phases by XRD. We are also grateful to Marc de Raféls, Laurent Emmanuel (Université Pierre et Marie Curie, Paris), Hugh Jenkyns and Ros Rickaby (Oxford University) for valuable discussions. Thanks are due to Anthony Cohen, another anonymous reviewer and Editor Peggy Delaney, who took part in the considerable improvement of an early version of the manuscript. The BRGM and Bruno Galbrun (CNRS, Paris) are acknowledged for providing access to the Sancerre–Couy cores. This work was partly supported by the National Research Fund of the Grand-Duchy of Luxembourg (MH) and a UPMC BQR action 2006 (FM).

Appendix A. Supplementary data

Supplementary data associated with this article can be found, in the online version, at doi:10.1016/j.epsl.2008.10.013.

References

- Bailey, T.R., Rosenthal, Y., McArthur, J.M., van de Schootbrugge, B., Thirlwall, M.F., 2003. Paleocceanographic changes of the Late Pliensbachian–Early Toarcian interval: a possible link to the genesis of an Oceanic Anoxic Event. *Earth Planet. Sci. Lett.* 212, 307–320.
- Bassoulet, J.P., Baudin, F., 1994. Le Toarcien inférieur: un épisode de crise dans les bassins et sur les plates-formes carbonatées de l'Europe du Nord-Ouest et de la Téthys. *Geobios, Mem. Spec.* 17, 645–654.
- Bassoulet, J.P., Elmi, S., Poisson, A., Cecca, F., Bellion, Y., Guiraud, R., Baudin, F., 1993. Middle Toarcian (184–182 Ma). In: Dercourt, J., Ricou, L.E., Vrielynck, B. (Eds.), *Atlas Tethys Paleoenvironmental Maps. Explanatory notes.* Gauthiers-Villards, Paris.

- Baudin, F., Herbin, J.P., Bassoulet, J.P., Decourt, J., Lachkar, G., Manivit, H., Renard, M., 1990. Distribution of organic matter during the Toarcian in the Mediterranean Tethys and Middle East. In: Huc, A.Y. (Ed.), *Deposition of Organic Facies*. AAPG Rev., pp. 73–91.
- Beerling, D.J., Brentnall, S.J., 2007. Numerical evaluation of mechanisms driving Early Jurassic changes in global carbon cycling. *Geology* 35, 247–250.
- Bour, I., Mattioli, E., Pittet, B., 2007. Nanofacies analysis as a tool to reconstruct palaeoenvironmental changes during the Early Toarcian anoxic event. *Palaeogeogr. Palaeoclimatol. Palaeoecol.* 249, 58–79.
- Bowen, G.J., Beerling, D.J., Koch, P.L., Zachos, J.C., Quattlebaum, T., 2004. A humid climate state during the Palaeocene/Eocene thermal maximum. *Nature* 432, 495–499.
- Bréhéret, J.G., Hanzo, M., El Albani, A., Iatzi, A., 2004. Impact de la vie benthique sur la genèse de nodules calcaires dans les black shales. *C. R. Geosci.* 336, 1355–1362.
- Çagatay, M.N., Borgowski, W.S., Ternois, Y.G., 2001. Factors affecting the diagenesis of Quaternary sediments at ODP Leg 172 sites in western North Atlantic: evidence from pore water and sediment geochemistry. *Chem. Geol.* 175, 467–484.
- Chandler, M.A., Rind, D., Ruedy, R., 1992. Pangaean climate during the Early Jurassic: GCM simulations and the sedimentary record of paleoclimate. *Geol. Soc. Amer. Bull.* 104, 543–559.
- Clarke, L.J., Jenkyns, H.C., 1999. New oxygen isotope evidence for long-term Cretaceous climatic change in the Southern hemisphere. *Geology* 27, 699–702.
- Cohen, A.S., Coe, A.L., Harding, S.M., Schwark, L., 2004. Osmium isotope evidence for the regulation of atmospheric CO₂ by continental weathering. *Geology* 32, 157–160.
- Cohen, A.S., Coe, A.L., Kemp, D.B., 2007. The Late Palaeocene–Early Eocene and Toarcian (Early Jurassic) carbon isotope excursions: a comparison of their time scales, associated environmental changes, causes and consequences. *J. Geol. Soc. (Lond.)* 164, 1093–1108.
- Dickens, G.R., O'Neil, J.R., Rea, D.C., Owen, R.M., 1995. Dissociation of oceanic methane hydrate as a cause of the carbon isotope excursion at the end of the Paleocene. *Paleoceanography* 10, 965–971.
- Duarte, L.V., Rodrigues, R., Dino, R., 2003. Carbon stable isotope analysis as a sequence stratigraphy tool. Case study from Lower Jurassic marly limestones of Portugal. IV South Amer. Symp. Isotope Geology, Salvador, pp. 341–344.
- Emmanuel, L., Renard, M., Cubaynes, R., Rafélis de, M., Herraño, M., Le Callonnec, L., Le Solleuz, A., Rey, J., 2006. Les schistes carbonés du Quercy (Tarn-France): la manifestation lithologique d'un événement de dissociation d'hydrates de méthane au cours du Toarcien. *Bull. Soc. Geol. Fr.* 177, 237–247.
- Erba, E., 2004. Calcareous nannofossils and Mesozoic oceanic anoxic events. *Mar. Micropaleontol.* 52, 85–106.
- Erba, E., Channell, J.E., Claps, T.M., Jones, C., Larson, R., Opdyke, B., Premoli Silva, I., Riva, A., Salvini, G., Torricelli, S., 1999. Integrated stratigraphy of the Cisono Apticore (southern Alps, Italy): a "reference section" for the Barremian–Aptian interval at low latitudes. *J. Foraminiferal Res.* 29, 371–391.
- Gély, J.P., Lorenz, C., Lorenz, J., 1996. Jurassic Formations in the Couy Borehole (Cher Department, France). Their detailed sequential analysis from the core sample descriptions and well-logging curves. *Rev. Inst. Fr. Pet.* 51, 319–331.
- Goy, G. (1979). Les « Schistes carbonés » (Toarcien inférieure) du Bassin de Paris en affleurements et en sondages. Étude par diagraphie, pétrographie, nanoflore calcaire, conditions de sédimentation. Unpublished PhD thesis, Université Pierre et Marie Curie, Paris, France, 187 pp.
- Gröcke, D.R., Rimmer, S.M., Yokosoulian, L.E., Cairncross, B., Tsikos, H., Hunen, J., accepted for publication. No evidence for thermogenic methane release in coal from Karoo-Ferrar large igneous province. *Earth Planet. Sci. Lett.*
- Hallam, A., 1983. Early and middle Jurassic molluscan biogeography and the establishment of the Central Atlantic Seaway. *Palaeogeogr. Palaeoclimatol. Palaeoecol.* 43, 181–193.
- Hallam, A., 1996. Recovery of the marine fauna in Europe after the end-Triassic and early Toarcian mass extinction. In: Hart, M.B. (Ed.), *Biotic Recovery from Mass Extinction Events*. *J. Geol. Soc. (Lond.)*, vol. 102, pp. 231–236.
- Hallam, A., 2001. A review of the broad pattern of Jurassic sea-level changes and their possible causes in the light of current knowledge. *Palaeogeogr. Palaeoclimatol. Palaeoecol.* 167, 23–37.
- Harries, P.J., Little, C.T.S., 1999. The early Toarcian (Early Jurassic) and the Cenomanian–Turonian (Late Cretaceous) mass extinctions: similarities and contrasts. *Palaeogeogr. Palaeoclimatol. Palaeoecol.* 154, 39–66.
- Hesselbo, S.P., Gröcke, D.R., Jenkyns, H.C., Bjerrum, C.J., Farrimond, P., Morgans Bell, H.S., Green, O.R., 2000. Massive dissociation of gas hydrate during a Jurassic oceanic event. *Nature* 406, 392–395.
- Hesselbo, S.P., Jenkyns, H.C., Duarte, L.V., Oliveira, L.C.V., 2007a. Carbon-isotope record of the Early Jurassic (Toarcian) Oceanic Anoxic Event from fossil wood and marine carbonate (Lusitanian Basin, Portugal). *Earth Planet. Sci. Lett.* 253, 455–470.
- Hesselbo, S.P., Jenkyns, H.C., Duarte, L.V., Oliveira, L.C.V., 2007b. Reply to comment on "Carbon-isotope record of the Early Jurassic (Toarcian) Oceanic Anoxic Event from fossil wood and marine carbonate (Lusitanian Basin, Portugal)". *Earth Planet. Sci. Lett.* 259, 640–641.
- Jenkyns, H.C., 1988. The early Toarcian (Jurassic) event: stratigraphy, sedimentary and geochemical evidence. *Am. J. Sci.* 288, 101–151.
- Jenkyns, H.C., 2003. Evidence for rapid climate change in the Mesozoic–Palaeogene greenhouse. *Philos. Trans.–Royal Soc., Math. Phys. Eng. Sci.* 361, 1885–1916.
- Jenkyns, H.C., Clayton, C.J., 1997. Lower Jurassic epicontinental carbonates and mudstones from England and Wales: chemostratigraphic signals and the early Toarcian anoxic event. *Sedimentology* 44, 687–706.
- Jenkyns, H.C., Gröcke, D.R., Hesselbo, S.P., 2001. Nitrogen isotope evidence for water mass denitrification during the early Toarcian (Jurassic) oceanic anoxic event. *Paleoceanography* 16, 593–603.
- Jenkyns, H.C., Jones, C.E., Gröcke, D.R., Hesselbo, S.P., Parkinson, D.N., 2002. Chemostratigraphy of the Jurassic System: applications, limitations and implications for palaeoceanography. *J. Geol. Soc. (Lond.)* 159, 351–378.
- Jiménez, A.P., Jiménez de Cisneros, C., Rivas, P., Vera, J.A., 1996. The early Toarcian anoxic event in the westernmost Tethys (Subbetic): paleogeographic and paleobiogeographic significance. *J. Geol.* 104, 399–416.
- Jones, C.E., Jenkyns, H.C., 2001. Seawater strontium isotopes, oceanic anoxic events, and seafloor hydrothermal activity in the Jurassic and Cretaceous. *Am. J. Sci.* 301, 112–149.
- Kálin, O., Bernoulli, D., 1984. Schizosphaerella Deflandre and Dangeard in Jurassic deeper-water carbonate sediments, Mazagan continental margin (Hole 547B) and Mesozoic Tethys. In: Hinz, K., Winterer, E.L., et al. (Eds.), *Initial Rep. DSDP*, vol. 79. U.S. Govt. Printing Office, Washington, pp. 437–448.
- Kemp, D.B., Coe, A.L., Cohen, A.S., Schwark, L., 2005. Astronomical pacing of methane release in the Early Jurassic period. *Nature* 437, 396–399.
- Küspert, W., 1982. Environmental changes during oil shale deposition as deduced from stable isotope ratios. In: Einsele, G., Seilacher, A. (Eds.), *Cyclic and Event Stratification*. Springer, Berlin, pp. 482–501.
- Lorenz, C., 1987. Forage scientifique de Sancerre-Couy (Cher). Rapport d'exécution et descriptions préliminaires. Terrains sédimentaires. Doc. Bur. rech. géol. min., Paris, vol. 136, p. 190.
- Lorenz, C., Lefavrais, A., Lorenz, J., Marchand, D., Million, R., 1991. Calage stratigraphique des diagraphies du Jurassique du sud du Bassin parisien à partir du sondage de Sancerre–Couy (Programme Géologie profonde de la France). *Bull. Soc. Geol. Fr.* 162, 947–952.
- Macchioni, F., Cecca, F., 2002. Biodiversity and biogeography of middle-late liassic ammonoids: implications for the Early Toarcian mass extinction. *Geobios, Mem. Spec.* 24, 165–175.
- Mailliot, S., Mattioli, E., Guex, J., Pittet, B., 2006. The Early Toarcian anoxia, a synchronous event in the Western Tethys? An approach by quantitative biochronology (Unitary Associations), applied on calcareous nannofossils. *Palaeogeogr. Palaeoclimatol. Palaeoecol.* 240, 562–586.
- Mattioli, E., Pittet, B., Bucefalo Palliani, R., Röhl, H.J., Moretini, E., 2004. Phytoplankton evidence for the timing and correlation of palaeoceanographical changes during the early Toarcian oceanic anoxic event (Early Jurassic). *J. Geol. Soc. (Lond.)* 161, 685–693.
- Mattioli, E., Pittet, B., Suan, G., Mailliot, S., 2008. Calcareous nannoplankton changes across the early Toarcian oceanic anoxic event in the western Tethys. *Paleoceanography* 23, PA3208. doi:10.1029/2007PA001435.
- McArthur, J.M., 2007. Comment on "Carbon-isotope record of the Early Jurassic (Toarcian) Oceanic Anoxic Event from fossil wood and marine carbonate (Lusitanian Basin, Portugal)" by Hesselbo S., Jenkyns H.C., Duarte L.V. and Oliveira L.C.V. *Earth Planet. Sci. Lett.* 259, 634–639.
- Meister, P., McKenzie, J.A., Warthmann, R., Vasconcelos, C., 2006. Mineralogy and petrography of diagenetic dolomite, Peru margin, ODP Leg 201. In: Jørgensen, B.B., D'Hondt, S.L., Miller, D.J. (Eds.), *Proc. ODP, Sci. Results*, p. 201.
- Mélières, F., 1991. Nature et origine des alternances métriques marnes-calcaires d'âge bajocien du forage de Sancerre–Couy (France). *Bull. Soc. Geol. Fr.* 162, 953–970.
- Minoletti, F., Gardin, S., Nicot, E., Renard, M., Spezzaferri, S., 2001. Mise au point d'un protocole expérimental de séparation granulométrique d'assemblages de nannofossiles calcaires: application paléocéologiques et géochimiques. *Bull. Soc. Geol. Fr.* 172, 437–446.
- Minoletti, F., Herraño, M., Gressier, V., in press. Separation of micron-sized sedimentary particles for palaeoceanography and calcareous nannofossil biogeochemistry. *Nature Protocols* 3–12. doi:10.1038/nprot.2008.200.
- Müller, P.J., Suess, E., 1979. Productivity, sedimentation rate and organic matter in the oceans. *Deep-Sea Res.* 26A, 1347–1362.
- Noël, D., Busson, G., 1991. L'importance des Schizosphères, Stomiosphères, *Conusphaera* et *Nannoconus* dans la genèse des calcaires fins pélagiques du Jurassique et du Crétacé inférieur. *Mem. Sci. Géol. Bull. (Strasbourg)* 43, 63–93.
- Paasche, E., 2002. A review of the coccolithophorid *Emiliania huxleyi* (Prymnesiophyceae), with particular reference to growth, coccolith formation, and calcification-photosynthesis interactions. *Phycologia* 40, 503–529.
- Pagani, M., Pedentchouk, N., Huber, M., Sluijs, A., Schouten, S., Brinkhuis, H., Sinninghe, J.S., Dickens, G.R., Expedition 302 Scientists, 2006. Arctic hydrology during global warming at the Palaeocene/Eocene thermal maximum. *Nature* 442. doi:10.1038/nature05043.
- Pálffy, J., Smith, P.L., 2000. Synchrony between Early Jurassic extinction, oceanic anoxic event, and the Karoo-Ferrar flood basalt volcanism. *Geology* 28, 747–750.
- Renard, M., 1985. Géochimie des carbonates pélagiques: mises en évidence des fluctuations de la composition des eaux océaniques depuis 140 M.A.: essai de chemostratigraphie. Doc. Bur. rech. géol. min., vol. 85, p. 650.
- Renard, M., Rafélis de, M., Emmanuel, L., Moullade, M., Masse, J.-P., Kuhnt, W., Bergen, J.A., Tronchetti, G., 2005. Early Aptian $\delta^{13}\text{C}$ and manganese anomalies from the historical Cassis-La Bédoule stratotype sections (S.E. France): relationship with a methane hydrate dissociation event and stratigraphic implications. *Notebooks on Geology*, article 2005/04 (CG2005_A04).
- Röhl, H.J., Schmid-Röhl, A., Oschmann, W., Frimmel, A., Schwark, L., 2001. The Posidonia Shale (Lower Toarcian) of SW-Germany: an oxygen-depleted ecosystem controlled by sea level and palaeoclimate. *Palaeogeogr. Palaeoclimatol. Palaeoecol.* 165, 27–52.
- Rosales, I., Quesada, S., Robles, S., 2001. Primary and diagenetic isotopic signals in fossils and hemipelagic carbonates: the Lower Jurassic of northern Spain. *Sedimentology* 48, 1149–1169.
- Sabatino, N., Neri, R., Bellanca, A., Jenkyns, H.C., Baudin, F., Parisi, G., Masetti, D., in press. Carbon-isotope records of the Early Jurassic (Toarcian) Oceanic Anoxic Event from the Valdorbia (Umbria Marche Apennines) and Monte Mangart (Julian Alps) sections: palaeoceanographic and stratigraphic implications. *Sedimentology*.
- Sælen, G., Doyle, P., Talbot, M.R., 1996. Stable-isotope analyses of belemnites rostra from the Whitby Mudstone Fm., England: surface water conditions during deposition of a marine Black Shale. *Palaio* 11, 97–117.

- Schlanger, S.O., Jenkyns, H.C., 1976. Cretaceous oceanic anoxic event: causes and consequences. *Geol. Mijnb.* 55, 179–184.
- Schmid-Röhl, A., Röhl, H.J., Oschmann, W., Schwark, L., 2002. Reconstruction du paléoenvironnement des schistes bitumineux épicontinentaux du Toarcien inférieur (schistes à posidonies dans le sud-ouest de l'Allemagne): facteurs de contrôle global ou régional? *Geobios* 35, 13–20.
- Scholle, P.A., Arthur, M.A., 1980. Carbon isotope fluctuations in Cretaceous pelagic limestones: potential stratigraphic and petroleum exploration tool. *AAPG Rev.* 64, 67–87.
- Schouten, S., Van Kaam-Peters, H.M.E., Rijpstra, W.I.C., Schoell, M., Sinninghe Damste, J.S., 2000. Effects of an oceanic event on the stable carbon isotopic composition of early Toarcian carbon. *Am. J. Sci.* 300, 1–22.
- Stoll, H.M., 2005. Limited range of interspecific vital effects in coccolith stable isotopic records during the Paleocene–Eocene thermal maximum. *Paleoceanography* 20, PA 1007. doi:10.1029/2004PA001046.
- Suan, G., Pittet, B., Bour, I., Mattioli, E., Duarte, L.V., Mailliot, S., 2008a. Duration of the Early Toarcian carbon isotope excursion deduced from spectral analysis: consequence for its possible causes. *Earth Planet. Sci. Lett.* 267, 666–679.
- Suan, G., Mattioli, E., Pittet, B., Mailliot, S., Lécuyer, C., 2008b. Evidence for major environmental perturbation prior to and during the Toarcian (Early Jurassic) Oceanic Anoxic Event from the Lusitanian Basin, Portugal. *Paleoceanography* 23, PA1202. doi:10.1029/2007PA001459.
- Suess, E., 1970. Interaction of organic compounds with calcium carbonate: I. Association phenomena and geochemical implications. *Geochim. Cosmochim. Acta* 34, 157–168.
- Tucker, M.E., Wright, V.P., 1990. *Carbonate Sedimentology*. Blackwell Scientific Publications, Oxford. 482 pages.
- Van Breugel, Y., Schouten, S., Paetzel, M., Nordeide, R., Sinninghe Damsté, J.S., 2005. The impact of recycling of organic carbon on the stable composition of dissolved inorganic carbon in a stratified marine system (Kyllaren fjord, Norway). *Org. Geochem.* 36, 1163–1173.
- Van Breugel, Y., Baas, M., Schouten, S., Mattioli, E., Sinninghe Damsté, J.S., 2006. Isorenieratane record in black shales from the Paris Basin, France: constraints on recycling of respired CO₂ as a mechanism for negative carbon isotope shifts during the Toarcian oceanic anoxic event. *Paleoceanography* 21, PA4220. doi:10.1029/2006PA001305.
- Van de Schootbrugge, B., McArthur, J.M., Bailey, T.R., Rosenthal, Y., Wright, J.D., Miller, K.G., 2005. Toarcian oceanic anoxic event: an assessment of global causes using belemnite C isotope records. *Paleoceanography* 20, PA 3008. doi:10.1029/2004PA001102.
- Weissert, H., Channell, J.E.T., 1989. Tethyan carbonate carbon isotope stratigraphy across the Jurassic–Cretaceous boundary. An indicator of decelerated global carbon cycling. *Paleoceanography* 4, 483–494.
- Weissert, H., Erba, E., 2004. Volcanism, CO₂ and paleoclimate: a Late Jurassic–Early Cretaceous carbon and oxygen isotope record. *J. Geol. Soc. (Lond.)* 161, 695–702.
- Wignall, P.B., 2001. Large igneous provinces and mass extinctions. *Earth-Sci. Rev.* 53, 1–33.
- Wignall, P.B., McArthur, J.M., Little, C.T.S., Hallam, A., 2006. Methane release in the Early Jurassic Period. *Nature* 441. doi:10.1038/nature04905.
- Woodfine, R.G., Jenkyns, H.C., Sarti, M., Baroncini, F., Violante, C., 2008. The response of two Tethyan carbonate platforms to the early Toarcian (Jurassic) oceanic anoxic event: environmental change and differential subsidence. *Sedimentology* 55, 1011–1028.